2014 47th Hawaii International Conference on System Science

Stochastic Optimal Power Flow with Uncertain Reserves from Demand Response

Maria Vrakopoulou, Johanna L. Mathieu, and Göran Andersson
Power Systems Laboratory, ETH Zürich, Switzerland
{*vrakopoulou, jmathieu, andersson*}*@eeh.ee.ethz.ch*

***Abstract*—Demand response (DR) can provide reserves in power systems but a fundamental challenge is that the amount of capacity available from DR is time-varying and uncertain. We propose a stochastic optimal power flow (OPF) formulation that handles uncertain energy from wind and uncertain reserves provided by DR. To handle the uncertainty, we formulate chance constraints and use a scenario based methodology to solve the stochastic OPF problem. This technique allows us to provide a-priori guarantees regarding the probability of constraint satisfaction. Additionally, we devise a strategy for the reserves, provided either by the generators or the loads, that could be deployed in real time operation. To evaluate the effectiveness of our methodology, we carry out a simulation-based analysis on the IEEE 30-bus network. Our case studies show that optimizing over the reserves provided by DR, even though they are uncertain, results in lower total cost compared to the case where only generation side reserves are taken into account. We also carry out a Monte Carlo analysis to empirically estimate the probability of constraint satisfaction and demonstrate that it is within the theoretical limits.**

I. Introduction

Reserve capacity is procured in electricity markets to ensure a match in supply and demand at each instant in time given uncertain consumption, production, and events such as line outages. To schedule energy and reserves using optimal power flow (OPF) formulations, we generally assume scheduled reserves are perfectly certain, i.e. that they will be available in real time if we need them. Some formulations take into account cases in which generators may be unable to provide scheduled reserves, for example, due to contingencies [1], [2]. However, new reserve resources, such as energy storage and demand response (DR), introduce different types of uncertainty than those considered in previous studies.

Research suggests that storage and DR could provide reserves in power systems [3], [4], [5]; however, the amount of reserves available may be time-varying and uncertain. This is especially true for DR in which both the load and the flexible portion of it may be a function of human behavior, ambient conditions such as weather, and past DR actions [6]. Therefore, for many types of loads, reserve capacity is difficult to estimate in real-time, and even harder to forecast because its based on other forecasted quantities. Moreover, it is often necessary to aggregate thousands of loads together to provide system-level reserves [7], [8] and at these scales it may be impossible to keep track of the time-varying capabilities and constraints of each load. Instead, we can use aggregated system models to approximate reserve capacity [8]; however, the mismatch between these models and the real system is another cause of uncertainty [6].

To mitigate reserve uncertainty, a DR aggregator could be conservative in offering reserves to power systems, making the reserves 'practically certain.' A better option may be to explicitly take reserve uncertainty into account in our planning algorithms, which should allow us to leverage more of the available resource. In this paper, we propose a stochastic optimal power flow (OPF) approach that allows us to consider uncertain reserves from DR. We model aggregations of DR resources as time-varying virtual energy storage units, and therefore must consider intertemporal energy constraints in the optimization problem. We assume DR could be used for both day-ahead hourly power scheduling and reserve scheduling. We formulate the problem as a probabilistic DC OPF with chance constraints and use a scenario based methodology [9], [10] to solve it. This approach allows us to provide probabilistic a-priori guarantees regarding the satisfaction of the system constraints.

This research builds on past work focused on methods to handle storage and uncertainty in OPF formulations. Ref. [11] formulated and proposed solution strategies for an OPF with distributed storage. The storage power and energy capacities are modeled as time-invariant, while in our paper we allow them to be time-varying. Several researchers have considered the problem of uncertain energy, for example, from wind power plants [12], [13], [2]. Refs. [14], [15], [16] use DR as reserves in stochastic OPFs with uncertain wind energy; however, the DR reserves are assumed certain. Ref. [17] proposes a formulation that allows uncertain aggregations of electric water heaters to provide a fixed amount of reserves. However, to our knowledge, ours is the first paper that determines the optimal amount of uncertain reserves within an OPF.

Our main contribution is to formulate a multi-stage day ahead probabilistic DC OPF that optimizes for uncertain reserves from DR and certain reserves from conventional generating units. More specifically, our formulation 1) results in the optimal reserve capacity offered by generators and controllable loads, 2) offers a strategy for reserve deployment in real time operation, 3) optimizes over tertiary reserve power that will relieve secondary frequency control reserves and bring the energy state of the controllable loads back to the scheduled value, and 4) provides a-priori guarantees that the proposed solution will be reliable with

978-1-4799-2504-9/14 $31.00 © 2014 IEEE
DOI 10.1109/HICSS.2014.296

a certain confidence, without requiring knowledge of the underlying distribution of the uncertainty variables.

To evaluate the effectiveness of our methodology, we carry out a simulation-based analysis on the IEEE 30-bus network [18]. This allows us to assess the costs associated with three OPF formulations in which we assume i) deterministic loads, ii) uncertain loads, and iii) uncertain but controllable loads that may be used for hourly scheduling and reserves. We also carry out a Monte Carlo analysis to empirically estimate the probability of constraint satisfaction.

The rest of the paper is organized as follows. In the next section, we detail the modeling of DR resources as uncertain reserves and describe the power flow assumptions. In Section III, we describe the stochastic optimization problem and discuss the scenario-based methodology we use to solve the resulting OPF. Section IV provides case studies, and in Section V we provide concluding remarks and discuss future research.

II. Modeling

A. Demand Response Resource Modeling

We assume that loads can shift their consumption in time but that the total amount of energy delivered to the load over a period of time is fixed. Therefore, we model aggregations of loads as virtual energy storage units [19]. Actions which decrease consumption relative to the baseline consumption (i.e. the consumption that would have occurred without scheduling) empty the storage unit and actions with increase consumption relative to the baseline consumption charge the storage unit. Therefore, the energy state S of the aggregation evolves as

$$S_{t+1} = S_t + (P_{C,t} - P_{T,t})\Delta\tau, \tag{1}$$

where $P_{C,t}$ is the mean power consumption of the controllable portion of the load at time step t and also the optimization variable, $P_{T,t}$ is the baseline consumption, and $\Delta\tau$ is the length of the time step.

Because the amount of controllable load within the system varies as a function of time, the size of the virtual energy storage unit is time-varying. Specifically, a unit's power and energy capacity are a function of a variety of time-dependent quantities such as ambient conditions and human behavior. Therefore, both P and S are constrained by time-varying quantities

$$\underline{P}_{C,t} \leqslant P_{C,t} \leqslant \overline{P}_{C,t}, \tag{2}$$

$$0 \leqslant S_t \leqslant \overline{S}_t, \tag{3}$$

where $\underline{P}_{C,t} + \overline{P}_{C,t}$ is the aggregate power capacity and $\overline{S}_t$ is the aggregate energy capacity. Ref. [19] describes a method of computing these capacities and P_T for an aggregation of residential electric space heaters or air conditioners as a function of outdoor air temperature T_t. Here, we use this method to compute $\overline{P}_C(T_t)$, $\overline{S}(T_t)$ and $P_T(T_t)$ for an aggregation of 1,000 heterogenous electric space heaters, as shown in Fig. 1. We assume $\underline{P}_C(T_t) = 0$ for all T_t.

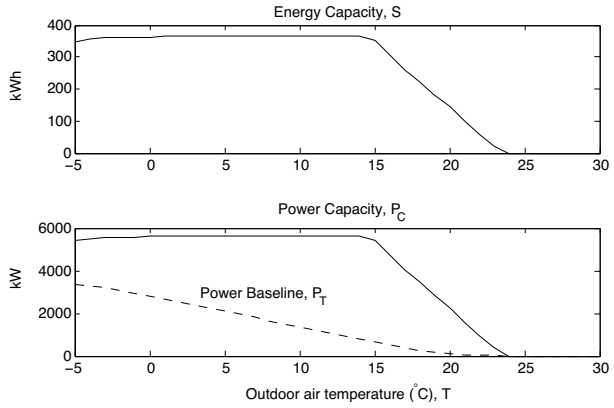

Figure 1. The power and energy capacity of an aggregation of electric heaters modeled as a virtual storage unit.

There are many reasons why $\overline{P}_C$, $\overline{S}$, and P_T may be uncertain including model error and forecasting error [6]. Here, we do not consider all sources of uncertainty but instead focus on just one cause: temperature forecasting error. Specifically, we assume that the values in Fig. 1 are accurate for a given outdoor air temperature but that our forecasts of outdoor air temperature are uncertain. Given a specific forecast of outdoor air temperature, we can use Fig. 1 as a look-up table to determine the expected power and energy capacity of a virtual storage unit for planning; however, the actual outdoor air temperature will dictate the actual capacities available in real-time. Note that even though we only consider this source of uncertainty in this paper, our OPF formulation works for cases in which we consider any and all sources of DR uncertainty.

B. Power Flow Modeling

In our framework, we use a DC OPF for day-ahead scheduling of hourly generator power set points P_G, controllable load set points P_C, secondary frequency control (also known as automatic generation control and load frequency control) capacities from both generators R_{GS} and controllable loads R_{LS}, and intra-hour re-dispatch capacities (e.g., tertiary control in Europe or intra-hour markets in the U.S.) from generators R_{GD}. Under the DC power flow assumption, the power flows across the lines are given by $P_l = AP_{inj}$, where $P_{inj} \in \mathbb{R}^{N_b}$ is the net power injection at the buses and A is a constant matrix that depends on the network admittances. This power flow representation results from eliminating the bus angles from the standard power flow equations as shown in [20]. It is an equivalent representation that allows for simpler manipulations of the network equations. We assume that both wind power production P_w and the controllable portion of the load (both its

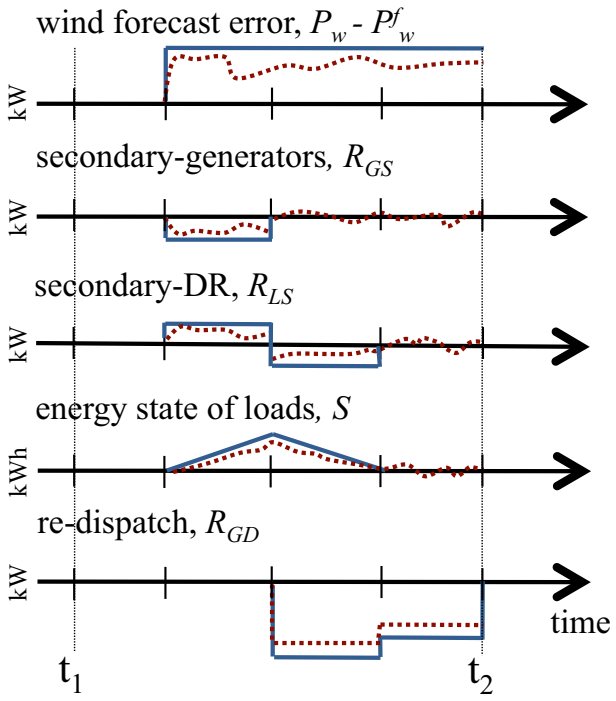

Figure 2. An example wind forecast error (top plot) and the corresponding actions of the secondary frequency controllers (second and third plot, with the fourth plot showing the energy state evolution of the loads used for secondary control) and re-dispatch (last plot), within one hour. The blue lines show the maximum wind forecast error and responses, which we plan for within the OPF. The red lines show a realistic wind forecast error and the responses. The secondary frequency controllers balance high frequency deviations while the re-dispatch is only able to produce constant outputs in each interval.

baseline and power/energy capacity, as defined in the last subsection) are uncertain. We always explicitly handle wind stochasticity within our probabilistic OPF formulation but we compare cases in which we do and do not handle load uncertainty and controllability. Specifically, we investigate three cases: i) deterministic loads, ii) uncertain loads, and iii) uncertain but controllable loads that can be used for both hourly scheduling and reserve provision.

We assume that each hour the intra-hour re-dispatch is activated four times, i.e. every fifteen minutes. Each 15-minute interval, the re-dispatch provides the amount of energy that would be required to return the controllable loads to the scheduled energy state (determined by the power setpoint) if the secondary frequency control signal were zero over that interval, which is similar to the method proposed by the California Independent System Operator [21]. Additionally, in each 15-minute interval, the re-dispatch covers the power mismatch between the expected generation and the actual generation. Figure 2 shows the action of the secondary frequency controllers and the re-dispatch for a given wind forecast error.

We do not consider security constraints in this paper for simplicity. However, our framework can be extended to also capture security constraints following the methodology of [2]. Therefore, here, secondary frequency control and re-dispatch are only needed to manage wind forecast errors. We assume reserve capacities are constant over one hour, and we size the secondary frequency control reserve capacity to cover a maximum wind power deviation over a period of 15 minutes. We size the intra-hour re-dispatch capacity to cover both the energy required by the loads and the wind power deviations.

III. Problem Formulation

A. Optimization problem

In this section, we formulate an OPF which considers uncertain but controllable loads, i.e. case iii) listed in the introduction. Note that the other cases we use for comparison in the case study, i.e. i) deterministic and uncontrollable loads and ii) uncertain and uncontrollable loads, are special cases of this formulation. The objective of the optimization problem is to determine the minimum cost generation dispatch, controllable load schedules, and reserve capacities provided by both generators and reserves.

We consider a power network of N_G generating units, N_w wind power plants, N_L loads, N_l lines, and N_b buses. Each load is comprised of an uncontrollable portion P_L, which is assumed known, and a controllable portion P_C, which is uncertain as described in Section II-A. We consider an optimization horizon $N_t = 24$ with hourly steps (i.e. $\Delta\tau = 1$) and introduce the subscript t in our notation to characterize the value of the corresponding quantities for a given time instance $t = 1, \ldots, N_t$. For each step t we define the vector of decision variables to be

$$\begin{aligned} x_t = [&P_{G,t},\ P_{C,t},\ R^{up}_{GS,t},\ R^{dn}_{GS,t},\ R^{up}_{LS,t},\ R^{dn}_{LS,t},\\ &R^{up}_{GD,t},\ R^{dn}_{GD,t},\ R^{up,0}_{GD,t},\ R^{dn,0}_{GD,t},\ d^{up}_{GS,t},\ d^{dn}_{GS,t},\\ &d^{up}_{LS,t},\ d^{dn}_{LS,t},\ d^{up,0}_{GD,t},\ d^{dn,0}_{GD,t},\ d^{up,1}_{GD,t},\ d^{dn,1}_{GD,t},\\ &d^{up,2}_{GD,t},\ d^{dn,2}_{GD,t}]^T \in \mathbb{R}^{15N_G+5N_L}. \end{aligned}$$

The vectors d are distribution vectors that distribute the generation-load mismatch to the resources that offer reserve capacity. The superscripts "up/dn" denote the increase/decrease of the produced or the consumed power of the generators or the loads, respectively. Hence, the up-regulating secondary reserves are characterized by the distribution vectors $d^{up}_{GS,t}$ and $d^{dn}_{LS,t}$ since the generators have to increase power while the loads have to decrease power. The total reserve capacity for up-regulating secondary reserves, for a given time step t, is given by $R^{up}_{GS,t} + R^{dn}_{LS,t}$. For the re-dispatch we use three sets of distribution vectors denoted by the superscripts "0,1,2", which are associated with 0) energy mismatches from the previous hour, 1) the intra-hour wind power mismatch, and 2) intra-hour energy mismatches.

More details on these decision variables will be given in the following paragraphs.

Let c denote cost. The optimization problem is

$$\min_{\{x_t\}_{t=1}^{N_t}} \sum_{t=1}^{N_t} \Big(c_1^T P_{G,t} + P_{G,t}^T [c_2] P_{G,t} + c_{GS,up}^T R_{GS,t}^{up} + c_{GS,dn}^T R_{GS,t}^{dn} \Big) + c_{LS,up}^T R_{LS,t}^{up} + c_{LS,dn}^T R_{LS,t}^{dn} \Big) + c_{GD,up}^T R_{GD,t}^{up} + c_{GD,dn}^T R_{GD,t}^{dn} \Big), \tag{4}$$

subject to

Deterministic constraints: All constraints presented below correspond to the forecast values, denoted with superscript f, of the wind power and temperature.

1) Power constraints: For all $t = 1, \ldots, N_t$,

$$\mathbf{1}_{1\times N_t} P_{inj,t} = 0, \tag{5}$$
$$-P_l \leqslant A P_{inj,t} \leqslant P_l, \tag{6}$$
$$\underline{P}_G \leqslant P_{G,t} \leqslant \overline{P}_G, \tag{7}$$
$$\underline{P}_C(T_t^f) \leqslant P_{C,t} \leqslant \overline{P}_C(T_t^f), \tag{8}$$

where

$$P_{inj,t} = C_G P_{G,t} + C_w P_{w,t}^f - C_L(P_{L,t} + P_{C,t}) \tag{9}$$

and the C matrices map the generator, wind, and load power vectors to the vector of bus injections. Constraint (5) guarantees power balance in the network, whereas (6), (7) encode the line and generation capacity limits, respectively. Constraint (8) imposes limits on the dispatch of the controllable portion of the load.

2) Energy Constraints: For all $t = 1, \ldots, N_t$,

$$0 \leqslant S_t \leqslant \overline{S}(T_t^f). \tag{10}$$

For all $t = 1, \ldots, N_t - 1$,

$$0 \leqslant S_{t+1} \leqslant \overline{S}(T_t^f), \tag{11}$$
$$S_{t+1} = S_t + (P_{C,t} - P_T(T_t^f))\Delta\tau. \tag{12}$$

Equation (12) shows the evolution of the energy state. Constraints (10), (11) are energy state capacity limits. They restrict the energy content at the beginning and at the end of hour t to lie within the energy state capacity limits of the specific hour. Due to the linearity of (12), requiring S_τ to satisfy the energy state limits for $\tau = t, t+1$ ensures that S_τ satisfies the energy limits for all $\tau \in [t, t+1]$.

Probabilistic constraints: For every $t = 1, \ldots, N_t$, the following constraints depend on the uncertainties, i.e. the wind power $P_{w,t}$ and the outdoor temperature T_t. We split the constraints into two parts. In part a), the wind power forecast error is compensated by the secondary frequency control offered both by the generators and DR for a period of at most 15 minutes, since re-dispatch occurs every 15 minutes. In part b), the constraints impose limitations on the operating point after a re-dispatch action is performed.

a) Secondary frequency control constraints:

1) Power constraints: For all $t = 1, \ldots, N_t$,

$$-P_l \leqslant A P_{inj,t} \leqslant P_l, \tag{13}$$
$$\underline{P}_G \leqslant P_{G,t} + R_{GS,t} \leqslant \overline{P}_G, \tag{14}$$
$$\underline{P}_C(T_t) \leqslant P_{C,t} + R_{LS,t} \leqslant \overline{P}_C(T_t), \tag{15}$$
$$-R_{GS,t}^{dn} \leqslant R_{GS,t} \leqslant R_{GS,t}^{up}, \tag{16}$$
$$-R_{LS,t}^{dn} \leqslant R_{LS,t} \leqslant R_{LS,t}^{up}, \tag{17}$$
$$R_{GS,t}^{dn}, R_{GS,t}^{up}, R_{LS,t}^{dn}, R_{LS,t}^{up} \geqslant 0, \tag{18}$$
$$\mathbf{1}_{1\times N_G} d_{GS,t}^{up} + \mathbf{1}_{1\times N_L} d_{LS,t}^{dn} = 1, \tag{19}$$
$$\mathbf{1}_{1\times N_G} d_{GS,t}^{dn} + \mathbf{1}_{1\times N_L} d_{LS,t}^{up} = 1, \tag{20}$$

where

$$P_{inj,t} = C_G(P_{G,t} + R_{GS,t}) + C_w P_{w,t} - C_L(P_{L,t} + P_{C,t} + R_{LS,t}), \tag{21}$$

$$R_{GS,t} = d_{GS,t}^{up} \max(-P_{m,t}, 0) - d_{GS,t}^{dn} \max(P_{m,t}, 0), \tag{22}$$

$$R_{LS,t} = d_{LS,t}^{up} \max(P_{m,t}, 0) - d_{LS,t}^{dn} \max(-P_{m,t}, 0), \tag{23}$$

$$P_{m,t} = \mathbf{1}_{1\times N_w}(P_{w,t} - P_{w,t}^f) - \mathbf{1}_{1\times N_L}(P_T(T_t) - P_T(T_t^f)). \tag{24}$$

Constraints (13)-(15) are similar to the deterministic constraints (6)-(8), with the difference being that due to the uncertainty, the generation and load schedules are adjusted by the power correction terms $R_{GS,t}$ and $R_{LS,t}$, respectively. With constraints (16)-(17), we determine the probabilistically worst case values of the power correction terms (given in (22)-(23)), which represent the reserves that are penalized in the objective function.

Following [2], the power correction terms $R_{GS,t}, R_{LS,t}$ in (22), (23) are defined as piecewise linear functions of the total mismatch between the generation and load. In our case, the mismatch is defined as the total wind power forecast error plus the total load forecast error (24). For example, for a negative wind power error only one of the terms

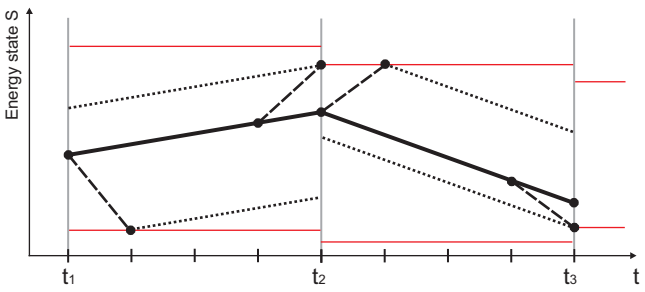

Figure 3. Evolution of the energy state of the loads. The solid lines correspond to the energy state trajectory for the case where the wind power is equal to its forecast (no reserves are needed in this case). Note that the energy state is not constant because the controllable load is dispatched above/below its baseline. The dashed lines show the evolution of the energy state for 15 minutes given that the maximum possible reserve capacity is deployed. The red lines show the capacity limits of each hour. In this paper, we assume that the lower energy bound is zero, but in principle that does not always have to be the case.

in (22), (23) will be active, providing up-regulating reserves. The distribution vectors that incorporated in this part of the formulation are $d^{up}_{GS,t}$, $d^{dn}_{GS,t}$, $d^{up}_{LS,t}$ and $d^{dn}_{LS,t}$. These vectors denote the fraction of the mismatch by which the generating units and the loads should adjust their production and consumption. Since the total mismatch is distributed both to the generating units and the loads, the sum of the elements of the corresponding up-regulating (respectively down-regulating) distribution vectors should be one. This is captured in (19), (20).

2) Energy Constraints: For all $t = 1, \dots, N_t$,

$$0 \leqslant S_t + (P_{C,t} + R_{LS,t} - P_T(T_t))\frac{\Delta\tau}{4} \leqslant \overline{S}(T_t), \tag{25}$$

$$0 \leqslant S_t + (P_{C,t} - P_T(T_t))\frac{3\Delta\tau}{4} + (P_{C,t} + R_{LS,t} - P_T(T_t))\frac{\Delta\tau}{4} \leqslant \overline{S}(T_t). \tag{26}$$

For all $t = 1, \dots, N_t - 1$,

$$0 \leqslant S_t + (P_{C,t} - P_T(T_t))\frac{3\Delta\tau}{4} + (P_{C,t} + R_{LS,t} - P_T(T_t))\frac{\Delta\tau}{4} \leqslant \overline{S}(T_{t+1}). \tag{27}$$

Constraints (25)-(27) are sufficient conditions that ensure that the energy state remains within the desired limits regardless of the time instance within $[t, t+1]$ when reserves are called upon. Due to the linear structure of the energy state dynamics, it suffices to satisfy the energy constraints for the first and last quarter of the hour. This can be also observed by inspection of Fig. 3. The solid lines correspond to the energy state trajectory for the case where the wind power is equal to its forecast (no reserves are needed in this case). The dashed lines show the evolution of the energy state for 15 minutes given that the maximum possible reserve capacity is deployed. The red lines denote the capacity limits of each hour.

b) Re-dispatch constraints:

1) Power constraints: For all $t = 1, \dots, N_t$,

$$-P_l \leqslant AP_{inj,t} \leqslant P_l, \tag{28}$$

$$\underline{P}_G \leqslant P_{G,t} + R_{GD,t} \leqslant \overline{P}_G, \tag{29}$$

$$\underline{P}_C(T_t) \leqslant P_{C,t} - R_{LS,t} \leqslant \overline{P}_C(T_t), \tag{30}$$

$$-R^{dn}_{GD,t} \leqslant R_{GD,t} \leqslant R^{up,}_{GD,t} \tag{31}$$

$$R^{dn}_{GD,t}, R^{up}_{GD,t} \geqslant 0, \tag{32}$$

$$\mathbf{1}_{1\times N_G} d^{up,1}_{GD,t} = 1, \tag{33}$$

$$\mathbf{1}_{1\times N_G} d^{dn,1}_{GD,t} = 1, \tag{34}$$

$$\mathbf{1}_{1\times N_G} d^{up,2}_{GD,t} = \mathbf{1}_{1\times N_L} d^{dn}_{LS,t}, \tag{35}$$

$$\mathbf{1}_{1\times N_G} d^{dn,2}_{GD,t} = \mathbf{1}_{1\times N_L} d^{up}_{LS,t}, \tag{36}$$

where

$$P_{inj} = C_G(P_{G,t} + R_{GD,t}) - C_L(P_{L,t} + P_{C,t} - R_{LS,t}) + C_w P_{w,t}, \tag{37}$$

$$R_{GD,t} = d^{up,1}_{GD,t}\max(-P_{m,t}, 0) - d^{dn,1}_{GD,t}\max(P_{m,t}, 0) + d^{up,2}_{GD,t}\max(-P_{m,t}, 0) - d^{dn,2}_{GD,t}\max(P_{m,t}, 0). \tag{38}$$

The constraints above ensure that the intra-hour re-dispatch satisfies both the network constraints and the load power limits. Note that the load set point $P_{C,t} - R_{LS,t}$ has an opposite term for the reserves compared to (15), which implies that the energy state returns to its scheduled trajectory (solid line in Fig. 3), thus satisfying the energy limits as well. Recall that the intra-hour re-dispatch capacity should cover both the energy required by the loads and the wind power deviations; this is captured in (33)-(36), (38). Specifically, the terms with the superscript '1' compensate the wind power error, whereas the terms with the superscript '2' compensate the energy required by the loads for providing secondary frequency control.

2) Coupling constraints: If at the end of an hour the energy state of the load has not returned to its scheduled value (determined by the power setpoint), the re-dispatch action of the following hour should cover this remaining energy in the first quarter. To capture this, for $t = 2, \dots, N_t$ we impose constraints (29)-(32), (37) with $R^0_{GD,t} + R_{GS,t}$ in place of $R_{GD,t}$, and require

$$-R^{dn}_{LS,t} \leqslant R_{LS,t} - R_{LS,t-1} \leqslant R^{up}_{LS,t}.$$

Moreover, we require the following power and energy constraints

$$0 \leqslant P_{C,t} - R_{LS,t-1} \leqslant \overline{P}_C(T_t), \tag{39}$$

$$0 \leqslant S_t + (P_{C,t} - P_T(T_t) + R_{LS,t} - R_{LS,t-1})\frac{\Delta\tau}{4} \leqslant \overline{S}(T_t), \quad (40)$$

where

$$R^0_{GD,t} = d^{up,0}_{GD,t}\max(-P_{m,t}, 0) - d^{dn,0}_{GD,t}\max(P_{m,t}, 0), \quad (41)$$

$$\mathbf{1}_{1\times N_G} d^{up,0}_{GD,t} = \mathbf{1}_{1\times N_L} d^{dn}_{LS,t-1}, \quad (42)$$

$$\mathbf{1}_{1\times N_G} d^{dn,0}_{GD,t} = \mathbf{1}_{1\times N_L} d^{up}_{LS,t-1}. \quad (43)$$

To facilitate the analysis of the next section, define $x = \{x_t\}_{t=1}^{N_t}$ to be a 'stacked' version of $\{x_t\}_{t=1}^{N_t}$ including all the decision variables, and let $\delta_t \in \mathbb{R}^{N_w+1}$ denote the uncertainty in step t, which here is the wind power $P_{w,t} \in \mathbb{R}^{N_w}$ and the temperature T_t. For every $t = 2, \ldots, N_t$, we require the constraints that are affected either by δ_t or by both δ_t and δ_{t-1} (for example, (39)) to be satisfied with probability at least $1 - \varepsilon_t$, where ε_t is a given violation level. Under this requirement, the aforementioned optimization problem can be formulated as a quadratic program with multiple chance constraints. Therefore, for every $t = 2, \ldots, N_t$, the probabilistic constraints can be written in compact notation:

$$\mathbb{P}\Big((\delta_t, \delta_{t-1}) \in \mathbb{R}^{N_w+1} \times \mathbb{R}^{N_w+1} \mid F(\delta_t, \delta_{t-1})x + g(\delta_t) \leqslant 0\Big) \geqslant 1 - \varepsilon_t, \quad (44)$$

where all matrices and vectors are of appropriate dimension. For $t = 1$, the chance constraint is similar to (44), with the difference that F depends only on δ_1 and the probability is with respect to the distribution of $\delta_1 \in \mathbb{R}^{N_w+1}$. In the next section, we show how to solve this problem without introducing assumptions on the probability distribution of the uncertainty and while providing guarantees regarding the probability of constraint satisfaction.

B. Solution approach

In [9], the authors introduce the 'scenario approach' to address chance constrained optimization problems. In this approach, the chance constraint is substituted with a finite number of hard constraints corresponding to different scenarios of the uncertainty vectors. By using a sufficient number of scenarios, the approach provides a-priori guarantees that the resulting solution satisfies the chance constraint with a certain confidence level. Here, we follow an alternative scenario-based methodology to deal with the chance constraint, which was proposed in [10] and extended in [22] to capture the case of multiple chance constraints.

This method includes two steps. In the first step, for each $t = 1, \ldots, N_t$, the scenario approach is used to determine, with a confidence of at least $1 - \beta_t$, the minimum volume set that contains at least $1 - \varepsilon_t$ probability mass of the uncertainty. Details on how to determine such a set can be found in [10], [2]. Here we denote this set by Δ_t. To compute this set, the number of scenarios we need to generate is given by [10]

$$N_t \geqslant \frac{1}{\varepsilon_t}\frac{e}{e-1}\Big(\ln\frac{1}{\beta_t} + 4(N_w + 1) - 1\Big). \quad (45)$$

In the second step, we use the probabilistically computed set Δ_t and formulate a robust problem where the uncertainty is confined in this set. For each $t = 2, \ldots, N_t$, the chance constraint (44) is substituted by the following robust constraint

$$F(\delta_t, \delta_{t-1})x + g(\delta_t) \leqslant 0, \text{ for all } (\delta_t, \delta_{t-1}) \in \Delta_t. \quad (46)$$

The interpretation of (46) is that the constraint should be satisfied for all values of $(\delta_t, \delta_{t-1}) \in \Delta_t$. For $t = 1$, the resulting constraint is similar with the difference that F depends only on δ_1 and we require the constraint to be satisfied for all $\delta_1 \in \Delta_1$. Following [10], [22], any feasible solution satisfying the robust constraints (46) will be feasible for each chance constraint (44) with a probability of at least $1 - \beta_t$. To solve the resulting robust program, the reader is referred to [23], [10].

IV. Case Studies

A. Data & error scenario generation

Error scenarios are generated under the assumption that the wind power in-feed and the temperature are independent, which allows us to use different models for each.

1) Wind data: We use normalized forecasted and actual hourly wind power data for Germany over the period 2006-2011. To generate the appropriate number of wind power scenarios, we use the Markov chain mechanism described in [24]. Specifically, we discretize the error between the forecast and the actual data to train a transition probability matrix, which we can then use to generate the scenarios. In our formulation, we assume that the wind error can come at any point during an hour, and persist for the rest of the hour, as shown in Fig. 2.

2) Temperature data: We generate temperature error scenarios using one year of forecasted and actual mean hourly temperature data from one weather station in Switzerland. Specifically, we generate 365 24-hour temperature error vectors and add these vectors to actual 24-hour temperature realizations to generate 24-hour temperature forecasts. This approach allows us to consider autocorrelation in the temperature errors over the course of the day; however, it does not allow us to take into account that the amount of error may be a function of the magnitude of the temperature.

We validate our approach using similar data from ten other weather stations in Switzerland. In Fig. 4, we plot histograms of the temperature errors in $\overline{P}_C$, $\overline{S}$, and P_T, generated with the data from all eleven weather stations. Note that the errors associated with $\overline{P}_C$ and $\overline{S}$ are highly non-Gaussian because of the shape of the curves in Fig. 1.

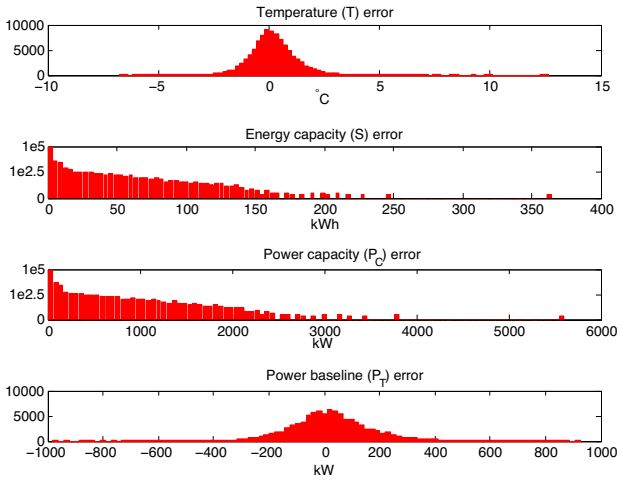

Figure 4. Histograms of the the errors associated with T, $\overline{P}_C$, $\overline{S}$, and P_T. Note the second and third plots are on a log scale.

Table I
COST PARAMETERS

generators	1	2	3	4	5	6
$c_{GS,up}$	6.00	6.75	7.00	5.25	5.00	5.00
$c_{GD,up}$	2.40	2.10	1.20	3.90	3.60	3.60

B. Simulation results

The methodology developed in the previous sections is applied to the IEEE 30-bus network [18], which is modified to include one wind power generator (i.e. $N_w = 1$) with capacity 35MW connected to bus 22. All loads were assumed partially controllable and therefore capable of being scheduled and providing reserves. Specifically, we assumed that over the course of a day 10% of the load, on average, is controllable and so we scaled each hour appropriately. Values for the generation cost vectors can be found in [18]. Table I provides the values for the up-regulating related cost vectors. The cost for the reserves provided by the loads is equal to 1.1 for all loads. The cost vectors for the down-regulating reserves are the same as the corresponding up-regulating ones. For our simulations, we used $\varepsilon_t = \varepsilon = 10\%$ and $\beta_t = \beta = 10^{-3}$ for all $t = 1, \ldots, N_t$. All optimization problems were solved using the solver CPLEX [25] via the MATLAB interface YALMIP [26].

Fig. 5 (upper plot) shows for each hour $t = 1, \ldots, N_t$ the maximum positive and negative wind power error computed from the scenarios, where the number of scenarios was determined in (45). To compensate a negative wind power error, up-regulating reserves are required, whereas for a positive wind power error down-regulating reserves need to be purchased. As shown in the middle plot of Fig. 5, these reserves are provided either by the secondary reserves from generating units, secondary reserves from DR, or by generator re-dispatch. The total reserve cost for each case, calculated as the sum of the corresponding up and down-regulating reserves, is shown in the lower plot of Fig. 5. As shown, the loads, despite their uncertainty, are chosen preferentially over the generators to provide secondary frequency control because of our cost assumptions. However, the generators need to provide a substantial amount of re-dispatch capacity. This division of services makes sense as generators are better suited to slower changes in their set points while load aggregations are better suited to fast, zero-mean deviations.

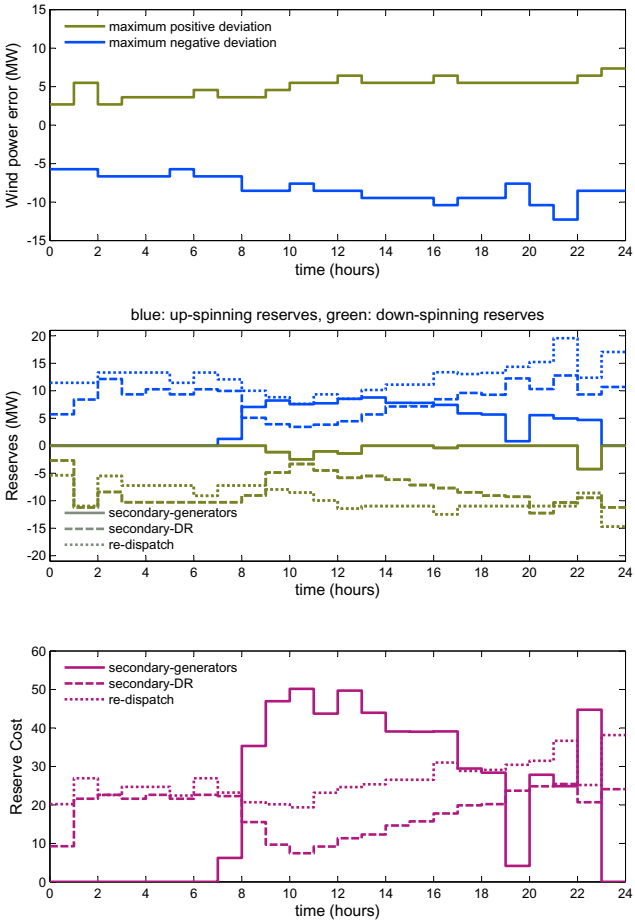

Figure 5. Upper plot: Maximum positive (green) and negative (blue) wind power error. Middle plot: Amount of reserve power provided by the secondary reserves of the generating units, the secondary reserves of DR, and by the re-dispatch. Lower plot: Total reserve cost for each case, calculated as the sum of the corresponding up and down-regulating reserves.

Fig. 6 (upper plot) shows the forecasted outdoor temperature as well as the temperature scenarios used in the optimization process. In the middle plot of Fig. 6, we show the optimal hourly schedule of the controllable portion of the load as computed by our algorithm, along with the forecasted consumption computed from the forecasted temperatures. Since the load's power capacity changes as a function of outdoor temperature, we show values corresponding to the

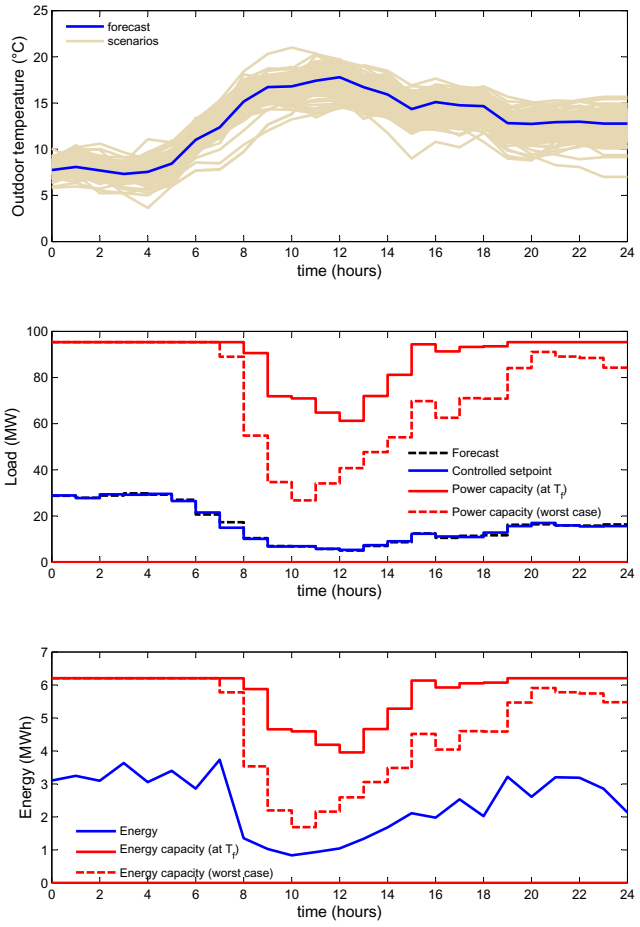

Figure 6. Upper plot: Scenarios and forecasted values of the outdoor temperature. Middle plot: Power of the controllable part of the load (solid blue), its forecast value (dashed black), and upper limits of the load power for the case where the temperature is equal to its forecast (solid red) and for the worst case (dashed red), respectively. Lower plot: Evolution of the load energy state. The interpretation of the individual lines is the same with those of the middle plot.

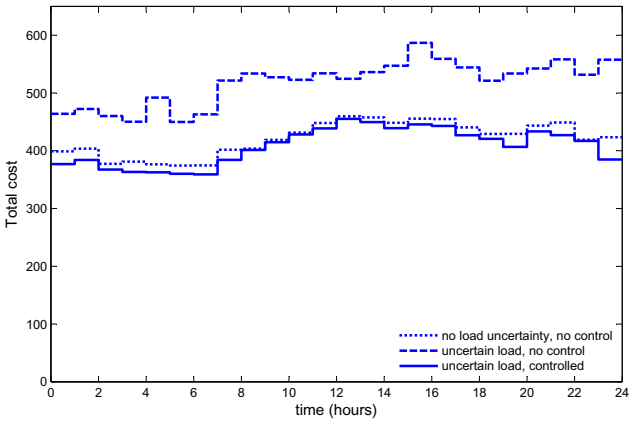

Figure 7. Total cost, calculated as the sum of the production and reserve costs, for three cases: 1) no load uncertainty (i.e. deterministic load), no control; 2) uncertain load, no control; and 3) uncertain but controllable load.

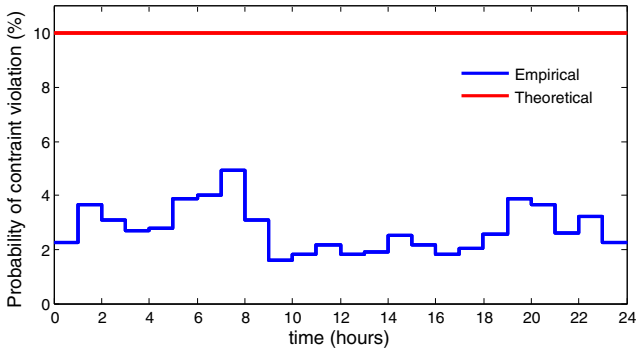

Figure 8. Empirical probability of constraint violation and the theoretical limit.

case when the temperature is equal to its forecast (solid red line) and the worse case error scenario (dashed red line). Note that when the temperature is low, the power capacity is high and nearly certain. The lower plot of Fig. 6 shows the evolution of the energy state of the load, and the interpretation of the lines is similar to that of the middle plot. As shown, the hourly schedule does not significantly deviate from the forecast; however, the additional power/energy capacity available can be used for secondary frequency control.

Fig. 7 shows the total cost of the solution generated by our approach, calculated as the sum of the production and reserve costs. For comparison purposes, we show the cost that would occur if the load was equal to its forecast value (deterministic) and no load controllability was taken into account. Additionally, we show the case where the load is not controllable, but is assumed to be uncertain (varying according to the scenarios of the upper plot of Fig. 6). This solution is higher cost than the deterministic case because we consider the load uncertainty within the OPF to ensure that the solution is robust. Note that the cost of the solution generated by our approach is always lower than the other values, highlighting the improvement resulting from incorporating load controllability in the reserve scheduling process.

To validate the guarantees offered by our approach regarding the probability of constraint satisfaction, we carried out a Monte Carlo analysis. Specifically, we fixed x to the optimal solution of our optimization problem and for each $t = 1, \ldots, N_t$ we computed the empirical probability of constraint violation. The latter was calculated as the fraction of 4,000 evaluation scenarios (different from those used in the optimization process) where at least one of the constraints inside the probability in (44) was violated. As shown in Fig. 8, this empirical estimate is below the theoretical ε_t guarantees for all $t = 1, \ldots, N_t$.

V. Concluding Remarks

We have demonstrated that uncertain reserves from DR could be considered in a day-ahead stochastic OPF to reduce the cost of dispatch. Considering uncertainty helps us be less conservative in committing DR resources to reserve markets. Therefore, our approach allows us to more-fully utilize the available DR resource, while still guaranteeing pre-defined levels of robustness. Importantly, the proposed scenario based methodology retains the structure of a deterministic problem (i.e. it remains a quadratic program) and hence is computationally tractable, and also amenable to distributed and decomposition based techniques.

Our results have important implications for the design of reserve markets. Specifically, we find that it is essential to have a mechanism to manage the energy state of load aggregations, which is in line with recent system operator proposals, for example [21]. We also find that it may be less important for a resource to be perfectly certain than to know its uncertainty so that that information can be incorporated within an OPF. Usually resources must demonstrate that they can accurately follow control signals to be able to participate in reserve markets; however, we instead suggest that the system operator should measure a range of a DR resource's abilities in order to understand both its expected response and error distribution.

Future work will concentrate on integrating N-1 security constraints into our framework. Additionally, we plan to explore distributed algorithms to ensure computational tractability even for realistically-sized networks. Moreover, to conduct a more realistic analysis, we aim to extend our models for generating uncertainty realizations to capture other sources of uncertainty (e.g., human behavior, model mismatch) and also the spatial correlation of the forecast error. We also plan to investigate the trade-offs between reserve uncertainty and costs.

References

[1] F. Bouffard and F. Galiana, "Stochastic security for operations planning with significant wind power generation," *IEEE Transactions on Power Systems*, vol. 23, no. 2, pp. 306–316, 2008.

[2] M. Vrakopoulou, K. Margellos, J. Lygeros, and G. Andersson, "A Probabilistic Framework for Reserve Scheduling and N-1 Security Assessment of Systems with High Wind Power Penetration," *IEEE Transactions on Power Systems*, 2013.

[3] D. Callaway and I. Hiskens, "Achieving controllability of electric loads," *Proceedings of the IEEE*, vol. 99, no. 1, pp. 184–199, 2011.

[4] I. Hiskens and D. Callaway, "Achieving controllability of plug-in electric vehicles," in *Vehicle Power and Propulsion Conference, 2009. VPPC '09. IEEE*, 2009, pp. 1215–1220.

[5] A. Gopstein, "Energy storage & the grid – from characteristics to impact," *Proceedings of the IEEE*, vol. 100, no. 2, pp. 311–316, 2012.

[6] J. Mathieu, M. González Vayá, and G. Andersson, "Uncertainty in the flexibility of aggregations of demand response resources," in *Proceedings of the Annual Meeting of the IEEE Industrial Electronics Society*, Vienna, Austria, 2013.

[7] D. Callaway, "Tapping the energy storage potential in electric loads to deliver load following and regulation, with application to wind energy," *Energy Conversion and Management*, vol. 50, pp. 1389–1400, 2009.

[8] J. Mathieu, S. Koch, and D. Callaway, "State estimation and control of electric loads to manage real-time energy imbalance," *IEEE Transactions on Power Systems*, vol. 28, no. 1, pp. 430–440, 2013.

[9] G. Calafiore and M. Campi, "The scenario approach to robust control design," *IEEE Transactions on Automatic Control*, vol. 51, no. 5, pp. 742–753, 2006.

[10] K. Margellos, P. Goulart, and J. Lygeros, "On the road between robust optimization and the scenario approach for chance constrained optimization problems," *submitted to IEEE Transactions on Automatic Control*, 2012.

[11] D. Gayme and U. Topcu, "Optimal power flow with distributed energy storage dynamics," in *American Control Conference*, 2011, pp. 1536–1542.

[12] A. Papavasiliou, S. Oren, and R. O'Neill, "Reserve requirements for wind power integration: a scenario-based stochastic programming framework," *IEEE Transactions on Power Systems*, vol. 26, no. 4, pp. 2197–2206, 2011.

[13] M. Vrakopoulou, K. Margellos, J. Lygeros, and G. Andersson, "A probabilistic framework for security constrained reserve scheduling of networks with wind power generation," in *Proceedings of IEEE EnergyCon*, 2012.

[14] T. Mount, L. Anderson, R. Zimmerman, and J. Cardell, "Coupling wind generation with controllable load and storage: A time-series application of the SuperOPF," Power System Engineering Research Center, Tech. Rep. PSERC 12-29, 2012.

[15] M. González Váya and G. Andersson, "Integrating renewable energy forecast uncertainty in smart-charging approaches for plug-in electric vehicles," in *Proceedings of PowerTech*, Grenoble, France, 2013.

[16] A. Papavasiliou and S. Oren, "A stochastic unit commitment model for integrating renewable supply and demand response," in *Proceedings of the IEEE PES General Meeting*, San Diego, CA, 2012.

[17] E. Vrettos and G. Andersson, "Combined load frequency control and active distribution network management with controllable loads," *to appear in the Proceedings of SmartGridComm*, 2013.

[18] R. D. Zimmerman, C. E. Murillo-Sanchez, and R. J. Thomas, "MATPOWER: Steady-state operations, planning, and analysis tools for power systems research and education," *IEEE Transactions on Power Systems*, vol. 26, no. 1, pp. 12–19, 2011.

[19] J. Mathieu, M. Kamgarpour, J. Lygeros, and D. Callaway, "Energy arbitrage with thermostatically controlled loads," in *Proceedings of the European Control Conference*, Zürich, Switzerland, 2013.

[20] M. Vrakopoulou, K. Margellos, J. Lygeros, and G. Andersson, "Probabilistic guarantees for the N-1 security of systems with wind power generation," *International Conference on Probabilistic Methods Applied to Power Systems*, 2012.

[21] California ISO, "Regulation energy management draft final proposal," January 2011. [Online]. Available: http://www.caiso.com/Documents/RevisedDraftFinalProposal-RegulationEnergyManagement-Jan13_2011.pdf

[22] X. Zhang, K. Margellos, P. Goulart, and J. Lygeros, "Stochastic Model Predictive Control Using a Combination of Randomized and Robust Optimization," *to appear in IEEE Conference on Decision and Control*, 2013.

[23] D. Bertsimas and M. Sim, "Tractable Approximations to Robust Conic Optimization Problems," *Mathematical Programming, Series B*, vol. 107, pp. 5–36, 2006.

[24] G. Papaefthymiou and B. Klöckli, "MCMC for wind power simulation," *IEEE Transactions on Energy Conversion*, vol. 23, no. 1, pp. 234–240, 2008.

[25] ILOG.SA., "CPLEX11.0 users manual," *Technical report, Gentilly, France*, 2008.

[26] J. Löfberg, "YALMIP: A toolbox for modeling and optimization in MATLAB," *IEEE International Symposium on Computer Aided Control Systems Design*, pp. 284–289, 2005.